

# Mean-field microrheology of a very soft colloidal suspension: inertia induces shear-thickening

Vincent Démery

*Department of Physics, University of Massachusetts, Amherst, MA 01003, USA*

*Laboratoire de Physico-Chimie Théorique, UMR CNRS Gulliver 7083, ESPCI, Paris, France*

## Abstract

Colloidal suspensions have a rich rheology and can exhibit shear-thinning as well as shear-thickening. Numerical simulations recently suggested that shear-thickening may be attributed to the inertia of the colloids, besides the hydrodynamic interactions between them. Here, we consider a dense bath of soft colloids following a Langevin dynamics and derive a mean-field equation for the colloidal density. We use this equation to get an analytical expression of the drag force felt by a probe pulled at constant velocity through the suspension. Our results show that inertia can indeed induce shear-thickening by allowing density waves to propagate through the suspension.

## 1 Introduction

Suspensions of colloids or droplets have a rich rheology [1, 2]. Whereas they can have a yield stress at volume fractions above the glass or jamming transitions [3], they behave as simple Newtonian fluids at moderate densities and small shear rates. Upon increasing the shear rate, their viscosity can then decrease (shear-thinning) or increase (shear-thickening) [4, 5].

Experimentally, the suspension rheology can be investigated using macrorheology or microrheology. In macrorheology, a global shear rate  $\dot{\gamma}$  is applied, and the resulting shear stress  $\tau$  is measured, the viscosity is then defined as  $\eta = \tau/\dot{\gamma}$  [6, 7]. In microrheology, the motion of a small probe in the medium is observed [8, 9]. Notably, in active microrheology, the probe is placed in an optical or magnetic trap and pulled at constant velocity  $v_p$  through the medium [10, 11, 12]. Measuring the drag force  $F_{\text{drag}}$  on the probe and the corresponding drag coefficient  $\lambda = F_{\text{drag}}/v_p$ , one can use the Stokes formula to deduce the viscosity:  $\lambda = 6\pi\eta a_p$ , where  $a_p$  is the radius of the probe. These two approaches have their theoretical counterpart both in numerical simulations ([3, 13, 14, 15] for macrorheology, [16, 17] for microrheology) and analytical computations ([6, 18] for macrorheology, [19, 20] for microrheology).

Shear-thinning, which is ubiquitous in experiments, is also present in most of the analytical computations both for dilute [19, 20] and dense suspensions [18, 21, 22, 23]. It is commonly associated with the disruption of the equilibrium microscopic structure, which gives the solution a large viscosity. On the other hand, various forms of shear-thickening exist and they are difficult to describe theoretically [5, 24]. While discontinuous shear-thickening may arise due to a dynamic jamming transition [25], a softer, continuous shear-thickening is induced by the formation of hydro-clusters due to the lubrication forces, which hold the particles together [26]. However, this mechanism has a negligible effect on soft-particles [5, 20, 27]: grafting polymer brushes to hard colloids can considerably delay shear-thickening [28].

A recent numerical work addressed the role of colloids inertia on the suspension rheology, and showed that it can induce shear-thickening as long as the system is sufficiently far from jamming [13]. In this article, we use the same ingredients – soft colloids, no hydrodynamic interactions – and provide an analytical derivation

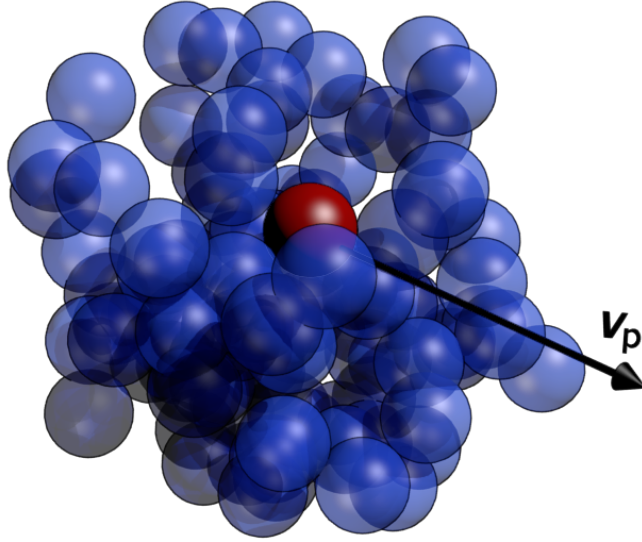


Figure 1: Illustration of the system studied: a probe (red) is pulled at constant velocity through a dense bath of soft colloids with inertia.

of this effect in the limit of very dense and soft colloids. Starting from the Langevin equation for the motion of the colloids, we derive an evolution equation for the bath density. This equation resembles one obtained previously [23], except that it is of second order in time due to inertia. Then, we use microrheology to investigate the properties of this medium: we compute the drag force felt by a probe pulled at constant velocity through the suspension (see Fig. 1). We obtain an analytical expression for the drag coefficient  $\lambda$ , which displays shear-thickening induced by inertia.

## 2 Model

We consider  $N$  colloids in a  $d$ -dimensional bath with positions  $\mathbf{x}_i(t)$  interacting via the pair potential  $V(\mathbf{x})$  and evolving according to Langevin dynamics, that we write in the form

$$m\ddot{\mathbf{x}}_i(t) + \lambda_s \dot{\mathbf{x}}_i(t) = \mathbf{F}_i(t) + \boldsymbol{\eta}_i(t), \quad (1)$$

where  $m$  is the mass of the colloids and  $\lambda_s$  the friction coefficient with the solvent. We can thus define the damping time associated to the particle inertia as

$$\tau = \frac{m}{\lambda_s}. \quad (2)$$

$\mathbf{f}_i(t)$  is the force on the particle  $i$  and  $\boldsymbol{\eta}_i(t)$  is the Gaussian white noise on the particle  $i$ . The noise is completely defined by its correlation function

$$\langle \boldsymbol{\eta}_i(t) \boldsymbol{\eta}_j(t')^T \rangle = 2T \lambda_s \delta_{ij} \delta(t - t') \mathbf{1}, \quad (3)$$

where  $T$  is the temperature (the Boltzmann constant is set to  $k_B = 1$ ). The force is given by the gradient of the potential created by the other colloids,

$$\mathbf{F}_i(t) = - \sum_j \partial_{\mathbf{x}_i} V(\mathbf{x}_i(t) - \mathbf{x}_j(t)). \quad (4)$$

The volume  $\mathcal{V}$  of the box containing the colloids is taken to infinity, keeping the density  $\rho_0 = N/\mathcal{V}$  constant.

A probe, which interacts with the bath colloids with the potential  $V_p(\mathbf{x})$ , is pulled at constant velocity  $\mathbf{v}_p$  through the suspension.

Without loss of generality, we can set the size of the probe  $a_p$ , the thermal energy  $T$  and the friction coefficient  $\lambda_s$  to 1 (we keep the temperature explicitly in our expressions to make the role of the temperature clear).

We focus on two quantities in the stationary regime:

- the drag force exerted by the colloids on the probe,
- the density of colloids around the probe.

In all the plots presented in this article, the dimension is set to  $d = 3$  and the pair potentials are Gaussian,

$$V(\mathbf{x}) = \frac{\epsilon}{(2\pi a^2)^{d/2}} \exp\left(-\frac{\mathbf{x}^2}{2a^2}\right), \quad (5)$$

$$V_p(\mathbf{x}) = \frac{\epsilon_p}{(2\pi)^{d/2}} \exp\left(-\frac{\mathbf{x}^2}{2}\right). \quad (6)$$

### 3 Main results and overview

#### 3.1 Main results

We show that, in the limit of very soft colloids (colloids that can overlap completely at a small energy cost), the bath density around the probe and the force on the probe can be computed analytically. The bath density in the reference frame of the probe is given in Fourier space by

$$\frac{\tilde{\delta\rho}^*(\mathbf{k})}{\rho_0} = \frac{-\mathbf{k}^2 \tilde{V}_p(\mathbf{k})}{\mathbf{k}^2(T + \rho_0 \tilde{V}(\mathbf{k})) - i\mathbf{v}_p \cdot \mathbf{k} - \tau(\mathbf{v}_p \cdot \mathbf{k})^2}, \quad (7)$$

where the star “\*” denotes the reference frame of the probe and  $\rho_0$  is the average density of colloids in the bath. This asymmetric density profile generates a drag  $\mathbf{F}_{\text{drag}} = -\lambda \mathbf{v}_p$ , where the drag coefficient  $\lambda$  is given by

$$\lambda = \rho_0 \int \frac{k_{\parallel}^2 \mathbf{k}^2 \tilde{V}_p(\mathbf{k})^2}{[\mathbf{k}^2(T + \rho_0 \tilde{V}(\mathbf{k})) - \tau(\mathbf{v}_p k_{\parallel})^2]^2 + (\mathbf{v}_p k_{\parallel})^2} \frac{dk}{(2\pi)^d}; \quad (8)$$

$k_{\parallel}$  is the component of the wavevector  $\mathbf{k}$  that is parallel to  $\mathbf{v}_p$ .

We distinguish two cases: in the first, the bath particles are much smaller than the probe,  $\tilde{V}(k \lesssim 1) = \tilde{V}(0)$ ; in the second, the bath particles are identical to the probe,  $V(\mathbf{x}) = V_p(\mathbf{x})$ . In the first case, we can define the Péclet number as [11]

$$\text{Pe} = \frac{v_p}{D_{\text{bath}}} = \frac{v_p}{T + \rho_0 \tilde{V}(0)} \quad (9)$$

and the rescaled drag  $D_{\text{bath}}^2 \lambda$  depends only on the Péclet number and the combination  $\tau D_{\text{bath}}$ :

$$D_{\text{bath}}^2 \lambda = \rho_0 \int \frac{k_{\parallel}^2 \mathbf{k}^2 \tilde{V}_p(\mathbf{k})^2}{[\mathbf{k}^2 - \tau D_{\text{bath}} \text{Pe}^2 k_{\parallel}^2]^2 + \text{Pe}^2 k_{\parallel}^2} \frac{dk}{(2\pi)^d}. \quad (10)$$

The bath density around the probe is plotted on Fig. 2 for different Péclet numbers. The rescaled drag coefficient is plotted as a function of the velocity for different values of  $\tau D_{\text{bath}}$  on Fig. 3. These flow curves exhibit shear-thickening, which is due to the inertia of the particles of the bath, in agreement with the results of Kawasaki et al. [13].

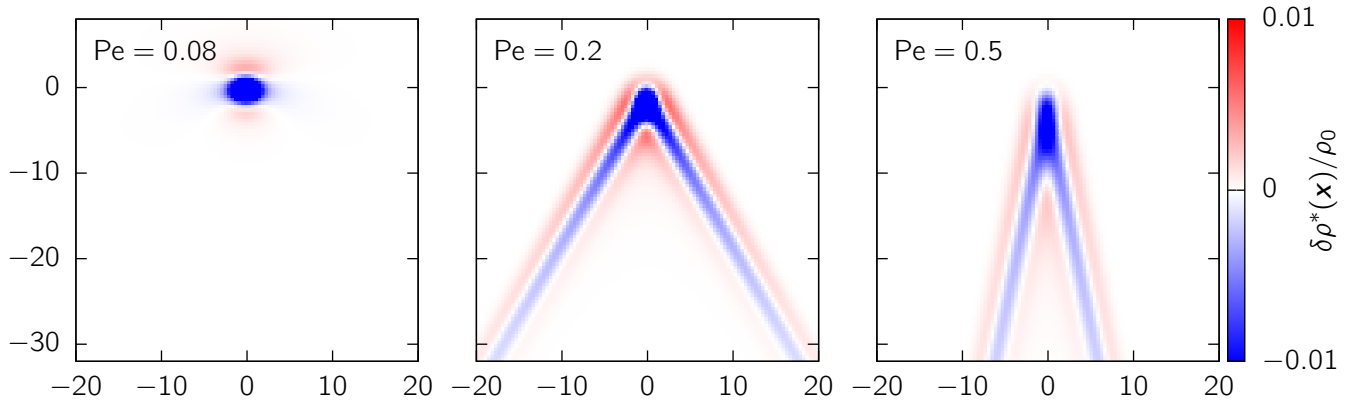


Figure 2: Bath density variations in the reference frame of the probe,  $\rho^*(x)/\rho_0 - 1$ , for different values of the Péclet number when the bath particles are point-like. The bath particles are heavy,  $\tau D_{\text{bath}} = 100$ .

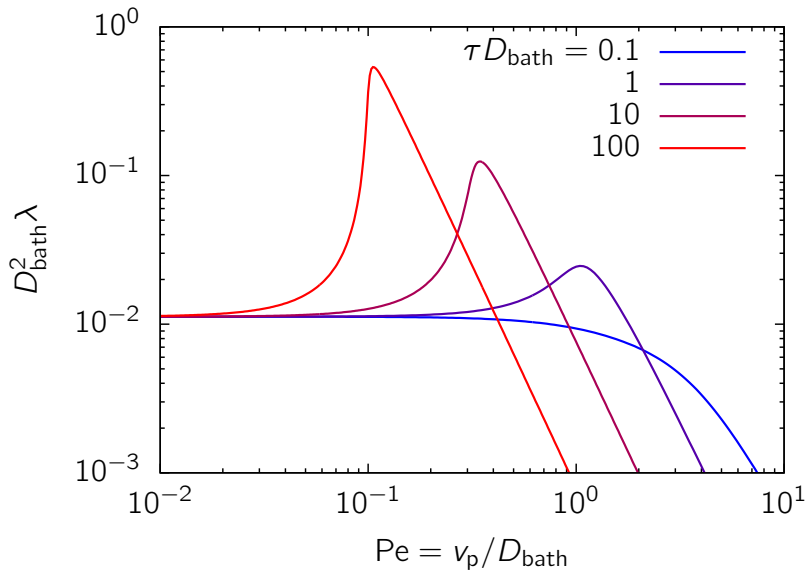


Figure 3: Rescaled friction coefficient for very small bath particles as a function of the Péclet number for different values of the parameter  $\tau D_{\text{bath}}$ .

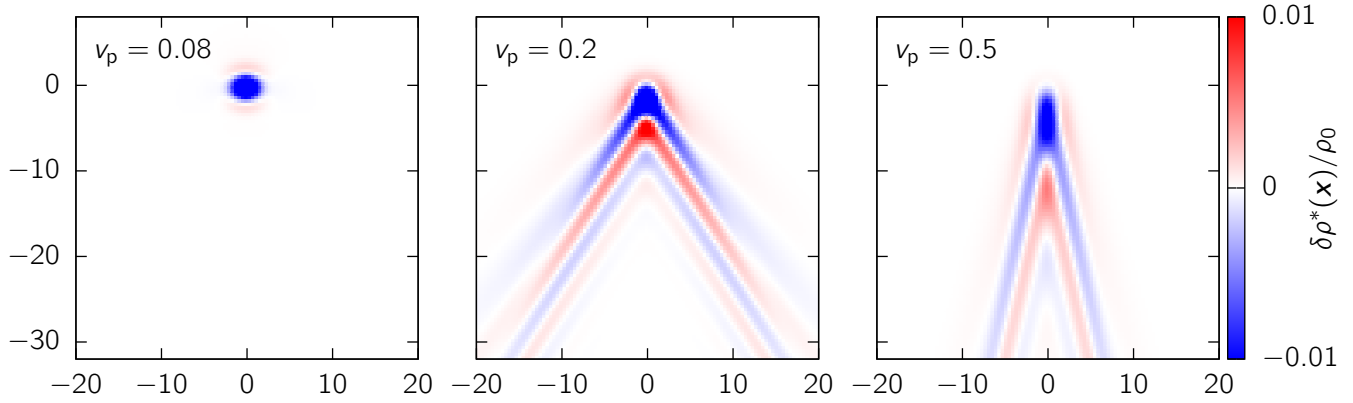


Figure 4: Bath density variations in the reference frame of the probe,  $\rho^*(x)/\rho_0 - 1$ , for different values of the probe velocity when the bath particles are identical to the probe. The bath particles are heavy,  $\tau = 100$ , and  $\rho_0\epsilon = 1$ .

On the other hand, when the bath particles are identical to the probe, there is no convenient way to define the Péclet number because the relaxation of the bath depends on the considered lengthscales; the inertia  $\tau$  of the bath colloids and the strength of the interactions between the colloids, characterized by  $\rho_0\epsilon$ , are independent parameters. However, the phenomenology does not change: the bath density around the probe has the same structure (see Fig. 4) and inertia induces shear-thickening (see Fig. 5).

### 3.2 Overview

Sec. 4 is devoted to the derivation of a linearized evolution equation for the bath density  $\rho(\mathbf{x}, t)$  that takes the inertia of the bath colloids into account. First, a Dean equation with inertia is derived, adapting the method used by Dean [29]; this equation rules the evolution of the density in the position-velocity space,  $f(\mathbf{x}, \mathbf{v}, t)$  (Subsec. 4.1). A closure approximation is used to obtain an equation for the density in the position space,  $\rho(\mathbf{x}, t)$  (Subsec. 4.2). Finally, the equation is linearized in the limit of high bath density and weak interactions, leading to Eq. 36 (Subsec. 4.3).

In Sec. 5, the linearized Dean equation with inertia, Eq. 36, is used to compute the response of the bath to the passage of a probe at constant velocity. The stationary bath density in the reference frame of the probe is computed (Subsec. 5.1, Eq. 43) and the drag felt by the probe is deduced (Subsec. 5.2, Eq. 48). The analytical expressions are computed numerically and discussed in Subsec. 5.3. Finally, our results are discussed in terms of the different timescales involved in the problem in Subsec. 5.4.

## 4 Derivation of the inertial Dean equation

### 4.1 Inertial equation in the position-velocity space

We can rewrite Eq. 1 as a system of two first order stochastic differential equations:

$$\dot{\mathbf{x}}_i(t) = \mathbf{v}_i(t), \quad (11)$$

$$\tau \dot{\mathbf{v}}_i(t) = -\mathbf{v}_i(t) + \mathbf{F}_i(t) + \boldsymbol{\eta}_i(t). \quad (12)$$

We follow the procedure used by Dean [29] to derive the evolution of the density

$$f(\mathbf{x}, \mathbf{v}, t) = \sum_i \delta(\mathbf{x} - \mathbf{x}_i(t)) \delta(\mathbf{v} - \mathbf{v}_i(t)) = \sum_i f_i(\mathbf{x}, \mathbf{v}, t), \quad (13)$$

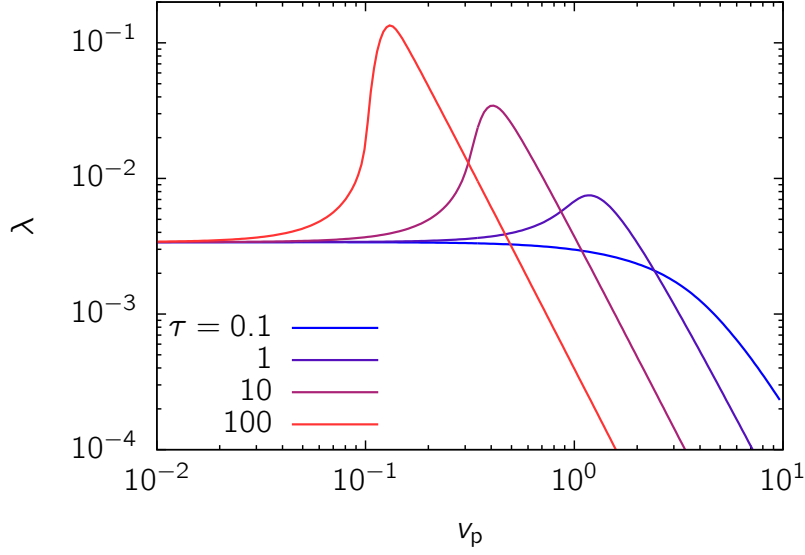


Figure 5: Friction coefficient as a function of the probe velocity when the bath particles are identical to the probe, for different values of the inertial relaxation time  $\tau$ , with  $\rho_0\epsilon = 1$ .

where  $f_i(\mathbf{x}, \mathbf{v}, t)$  is the density associated with the particle  $i$ . We consider an arbitrary function  $g(\mathbf{x}, \mathbf{v})$ . Applying this to a particle coordinates, it may be written

$$g(\mathbf{x}_i(t), \mathbf{v}_i(t)) = \int f_i(\mathbf{x}, \mathbf{v}, t) g(\mathbf{x}, \mathbf{v}) d\mathbf{x} d\mathbf{v}, \quad (14)$$

We now write the total time derivative of  $g(\mathbf{x}_i(t), \mathbf{v}_i(t))$  in two ways. First, we use the time derivative of the density,

$$\frac{d}{dt} [g(\mathbf{x}_i(t), \mathbf{v}_i(t))] = \int \partial_t f_i(\mathbf{x}, \mathbf{v}, t) g(\mathbf{x}, \mathbf{v}) d\mathbf{x} d\mathbf{v}. \quad (15)$$

Second, using stochastic calculus [30],

$$\begin{aligned} \frac{d}{dt} [g(\mathbf{x}_i(t), \mathbf{v}_i(t))] &= \mathbf{v}_i(t) \cdot \partial_{\mathbf{x}} g(\mathbf{x}_i(t), \mathbf{v}_i(t)) \\ &+ \frac{1}{\tau} [-\mathbf{v}_i(t) + \mathbf{F}_i(t) + \boldsymbol{\eta}_i(t)] \cdot \partial_{\mathbf{v}} g(\mathbf{x}_i(t), \mathbf{v}_i(t)) \\ &+ \frac{T}{\tau^2} \partial_{\mathbf{v}}^2 g(\mathbf{x}_i(t), \mathbf{v}_i(t)), \end{aligned} \quad (16)$$

where the right hand side can be written in term of the density, as

$$\begin{aligned} \frac{d}{dt} [g(\mathbf{x}_i(t), \mathbf{v}_i(t))] &= \int f_i(\mathbf{x}, \mathbf{v}, t) \left[ \mathbf{v} \cdot \partial_{\mathbf{x}} g(\mathbf{x}, \mathbf{v}) \right. \\ &+ \frac{1}{\tau} [\mathbf{v} + \mathbf{F}_i(t) + \boldsymbol{\eta}_i(t)] \cdot \partial_{\mathbf{v}} g(\mathbf{x}, \mathbf{v}) \\ &+ \left. \frac{T}{\tau^2} \partial_{\mathbf{v}}^2 g(\mathbf{x}, \mathbf{v}) \right] d\mathbf{x} d\mathbf{v}. \end{aligned} \quad (17)$$

Integration by parts allows to identify Eqs. 15 and 17 to get the derivative of the density

$$\begin{aligned} \partial_t f_i(\mathbf{x}, \mathbf{v}, t) &= -\mathbf{v} \cdot \partial_{\mathbf{x}} f_i(\mathbf{x}, \mathbf{v}, t) + \frac{1}{\tau} \partial_{\mathbf{v}} \cdot \left[ \left( \mathbf{v} + \sum_j \partial_{\mathbf{x}} V(\mathbf{x} - \mathbf{x}_j(t)) - \boldsymbol{\eta}_i(t) \right) f_i(\mathbf{x}, \mathbf{v}, t) \right] \\ &+ \frac{T}{\tau^2} \partial_{\mathbf{v}}^2 f_i(\mathbf{x}, \mathbf{v}, t). \end{aligned} \quad (18)$$

Summing the evolution of the densities of all the particles,  $f = \sum_i f_i$ , leads to

$$\begin{aligned} \partial_t f(\mathbf{x}, \mathbf{v}, t) = & -\mathbf{v} \cdot \partial_{\mathbf{x}} f(\mathbf{x}, \mathbf{v}, t) + \frac{1}{\tau} \partial_{\mathbf{v}} \cdot \left[ \left( \mathbf{v} + \int \partial_{\mathbf{x}} (V *_{\mathbf{x}} f)(\mathbf{x}, \mathbf{v}', t) d\mathbf{v}' \right) f(\mathbf{x}, \mathbf{v}, t) \right] \\ & + \frac{T}{\tau^2} \partial_{\mathbf{v}}^2 f(\mathbf{x}, \mathbf{v}, t) - \frac{1}{\tau} \partial_{\mathbf{v}} \cdot \left[ \sum_i f_i(\mathbf{x}, \mathbf{v}, t) \boldsymbol{\eta}_i(t) \right]. \end{aligned} \quad (19)$$

$*_{\mathbf{x}}$  is the convolution with respect to the  $\mathbf{x}$  variable:  $(V *_{\mathbf{x}} f)(\mathbf{x}, \mathbf{v}, t) = \int V(\mathbf{x} - \mathbf{x}') f(\mathbf{x}', \mathbf{v}, t) d\mathbf{x}'$ . The noise term

$$\xi(\mathbf{x}, \mathbf{v}, t) = -\partial_{\mathbf{v}} \cdot \left[ \sum_i f_i(\mathbf{x}, \mathbf{v}, t) \boldsymbol{\eta}_i(t) \right] \quad (20)$$

is shown in [29] to be statistically equivalent to

$$\xi'(\mathbf{x}, \mathbf{v}, t) = \partial_{\mathbf{v}} \cdot \left[ f(\mathbf{x}, \mathbf{v}, t)^{1/2} \boldsymbol{\eta}(\mathbf{x}, \mathbf{v}, t) \right], \quad (21)$$

where the vector field  $\boldsymbol{\eta}(\mathbf{x}, \mathbf{v}, t)$  as a correlation function

$$\langle \boldsymbol{\eta}(\mathbf{x}, \mathbf{v}, t) \boldsymbol{\eta}(\mathbf{x}', \mathbf{v}', t')^T \rangle = 2T \delta(\mathbf{x} - \mathbf{x}') \delta(\mathbf{v} - \mathbf{v}') \delta(t - t') \mathbf{1}. \quad (22)$$

This allows to write the Dean equation with inertia in its final form:

$$\begin{aligned} \partial_t f(\mathbf{x}, \mathbf{v}, t) = & -\mathbf{v} \cdot \partial_{\mathbf{x}} f(\mathbf{x}, \mathbf{v}, t) + \frac{1}{\tau} \partial_{\mathbf{v}} \cdot \left[ \left( \mathbf{v} + \int \partial_{\mathbf{x}} (V *_{\mathbf{x}} f)(\mathbf{x}, \mathbf{v}', t) d\mathbf{v}' \right) f(\mathbf{x}, \mathbf{v}, t) \right] \\ & + \frac{T}{\tau^2} \partial_{\mathbf{v}}^2 f(\mathbf{x}, \mathbf{v}, t) + \frac{1}{\tau} \partial_{\mathbf{v}} \cdot \left[ f(\mathbf{x}, \mathbf{v}, t)^{1/2} \boldsymbol{\eta}(\mathbf{x}, \mathbf{v}, t) \right]. \end{aligned} \quad (23)$$

## 4.2 Closure and equation in the position space only

We aim at obtaining an equation for the position density

$$\rho(\mathbf{x}, t) = \int f(\mathbf{x}, \mathbf{v}, t) d\mathbf{v}. \quad (24)$$

Integrating Eq. 23 over the velocity leads to

$$\partial_t \rho(\mathbf{x}, t) = -\partial_{\mathbf{x}} \cdot \mathbf{j}(\mathbf{x}, t), \quad (25)$$

where we introduced the current

$$\mathbf{j}(\mathbf{x}, t) = \int \mathbf{v} f(\mathbf{x}, \mathbf{v}, t) d\mathbf{v}. \quad (26)$$

The evolution of the current can be obtained by multiplying Eq. 23 by the velocity and integrating over the velocity; this gives

$$\begin{aligned} \partial_t \mathbf{j}(\mathbf{x}, t) = & -\partial_{\mathbf{x}\alpha} \left[ \int v^\alpha \mathbf{v} f(\mathbf{x}, \mathbf{v}, t) d\mathbf{v} \right] - \frac{1}{\tau} [\mathbf{j}(\mathbf{x}, t) + \rho(\mathbf{x}, t) \partial_{\mathbf{x}} (V * \rho)(\mathbf{x}, t)] \\ & - \frac{1}{\tau} \int f(\mathbf{x}, \mathbf{v}, t)^{1/2} \boldsymbol{\eta}(\mathbf{x}, \mathbf{v}, t) d\mathbf{v}. \end{aligned} \quad (27)$$

A summation over  $\alpha$  is implicit in the first term, and we omitted the index  $\mathbf{x}$  in the convolution. The correlation of the noise term can be computed:

$$\begin{aligned} \left\langle \left( \int f(\mathbf{x}, \mathbf{v}, t)^{1/2} \boldsymbol{\eta}(\mathbf{x}, \mathbf{v}, t) d\mathbf{v} \right) \left( \int f(\mathbf{x}', \mathbf{v}', t')^{1/2} \boldsymbol{\eta}(\mathbf{x}', \mathbf{v}', t') d\mathbf{v}' \right)^T \right\rangle \\ = 2T \delta(\mathbf{x} - \mathbf{x}') \delta(t - t') \int f(\mathbf{x}, \mathbf{v}, t) d\mathbf{v} \\ = 2T \delta(\mathbf{x} - \mathbf{x}') \delta(t - t') \rho(\mathbf{x}, t). \end{aligned} \quad (28)$$

Thus, the noise can be written as  $\rho(\mathbf{x}, t)^{1/2}\bar{\boldsymbol{\eta}}(\mathbf{x}, t)$ , where the Gaussian white vector noise  $\bar{\boldsymbol{\eta}}(\mathbf{x}, t)$  has the correlation function

$$\langle \bar{\boldsymbol{\eta}}(\mathbf{x}, t)\bar{\boldsymbol{\eta}}(\mathbf{x}', t')^\top \rangle = 2T\delta(t-t')\delta(\mathbf{x}-\mathbf{x}')\mathbf{1}. \quad (29)$$

The first term on the r.h.s of Eq. 27 is problematic, because it involves the second moment in the velocity of the distribution  $f(\mathbf{x}, \mathbf{v}, t)$ . A closure should be used in order to get an equation for the position density only. The equilibrium solution of Eq. 23 without noise is the Maxwell distribution

$$f_{\text{eq}}(\mathbf{x}, \mathbf{v}, t) = \rho_0 \left(2\pi\frac{T}{\tau}\right)^{-d/2} \exp\left(-\frac{\tau\mathbf{v}^2}{2T}\right). \quad (30)$$

The second moment of this distribution for the velocity is

$$\int \mathbf{v}\mathbf{v}^\top f_{\text{eq}}(\mathbf{x}, \mathbf{v}, t)d\mathbf{v} = \frac{T}{\tau}\rho_0\mathbf{1}. \quad (31)$$

We use this equilibrium average to write the second moment in the velocity as a function of the density only:

$$\int \mathbf{v}\mathbf{v}^\top f(\mathbf{x}, \mathbf{v}, t)d\mathbf{v} \simeq \frac{T}{\tau}\rho(\mathbf{x}, t)\mathbf{1}. \quad (32)$$

The fact that the second moment in the velocity does not depend on the current is a strong assumption. However, this relation can be justified for the linearized version of the density evolution presented in the next subsection (see App. A).

With this closure relation, the evolution of the current can be written as

$$\partial_t \mathbf{j}(\mathbf{x}, t) = -\frac{T}{\tau}\partial_x \rho(\mathbf{x}, t) - \frac{1}{\tau}\mathbf{j}(\mathbf{x}, t) - \frac{1}{\tau}\rho(\mathbf{x}, t)\partial_x(V * \rho)(\mathbf{x}, t) - \frac{1}{\tau}\rho(\mathbf{x}, t)^{1/2}\bar{\boldsymbol{\eta}}(\mathbf{x}, t)d\mathbf{v}. \quad (33)$$

Taking the divergence of this equation and using the density conservation Eq. 25 leads to a second order equation for the density only

$$\tau\partial_t^2 \rho(\mathbf{x}, t) + \partial_t \rho(\mathbf{x}, t) = T\partial_x^2 \rho(\mathbf{x}, t) + \partial_x \cdot [\rho(\mathbf{x}, t)\partial_x(V * \rho)(\mathbf{x}, t)] + \partial_x \cdot \left[\rho(\mathbf{x}, t)^{1/2}\bar{\boldsymbol{\eta}}(\mathbf{x}, t)\right]. \quad (34)$$

This equation differs from the over-damped Dean equation [29] only by the second time derivative of the density on the left hand side. The only approximation used is the closure 32.

### 4.3 Linearized equation for the position density

The equation 34 for the density  $\rho(\mathbf{x}, t)$  is non linear and contains a multiplicative noise, which make its analytical treatment difficult. These difficulties can be circumvented if the bath is dense, in which case Eq. 34 can be linearized around a uniform density  $\rho_0$  [23]. The density is decomposed in a uniform part and a small fluctuating part,

$$\rho(\mathbf{x}, t) = \rho_0 + \rho_0^{1/2}\psi(\mathbf{x}, t). \quad (35)$$

In the limit of a dense bath with a weak interaction,  $\rho_0 \rightarrow \infty$  and  $\rho_0 V(\mathbf{x}) \rightarrow \mathcal{V}(\mathbf{x})$ , the resulting equation for the density fluctuation  $\psi(\mathbf{x}, t)$  is (see Eq. 21 in [23]):

$$\tau\partial_t^2 \psi(\mathbf{x}, t) + \partial_t \psi(\mathbf{x}, t) = T\partial_x^2 \psi(\mathbf{x}, t) + \partial_x^2 [(\mathcal{V} * \psi)(\mathbf{x}, t)] + \partial_x \cdot \bar{\boldsymbol{\eta}}(\mathbf{x}, t). \quad (36)$$

This equation is the main result of this section, it allows to compute the drag force felt by the probe analytically, as we shall see in the next section.

## 5 Application to a probe pulled at constant velocity

### 5.1 Bath density around the probe

In order to assess the rheological properties of the suspension, instead of shearing the material globally, as is done in [13], we pull a probe particle at constant velocity  $\mathbf{v}_p$  through the medium, as in [31]. The interaction between the probe and a particle of the bath is given by the potential  $V_p(\mathbf{x}) = \mathcal{V}_p(\mathbf{x})/\rho_0$ .

The effect of the probe on the density field can be incorporated in the linearized equation 36 as in [23],

$$\begin{aligned} \tau \partial_t^2 \psi(\mathbf{x}, t) + \partial_t \psi(\mathbf{x}, t) = & T \partial_x^2 \psi(\mathbf{x}, t) + \partial_x^2 [(\mathcal{V} * \psi)(\mathbf{x}, t)] + \partial_x \cdot \bar{\boldsymbol{\eta}}(\mathbf{x}, t) \\ & + \rho_0^{-1/2} \partial_x^2 [\mathcal{V}_p(\mathbf{x} - \mathbf{x}_p(t))], \end{aligned} \quad (37)$$

where  $\mathbf{x}_p(t) = \mathbf{v}_p t$  is the position of the probe. Conversely, the force exerted by the bath particles on the probe is

$$\mathbf{F}(t) = -\rho_0^{-1/2} \partial_x [(\mathcal{V}_p * \psi)(\mathbf{x}_p(t), t)]. \quad (38)$$

We are interested in the average stationary solution for the field in the reference frame of the particle,

$$\psi^*(\mathbf{x}) = \langle \psi(\mathbf{x} + \mathbf{v}_p t, t) \rangle; \quad (39)$$

it satisfies

$$\tau(\mathbf{v}_p \cdot \partial_x)^2 \psi^*(\mathbf{x}) - \mathbf{v}_p \cdot \partial_x \psi^*(\mathbf{x}) = T \partial_x^2 \psi^*(\mathbf{x}) + \partial_x^2 (\mathcal{V} * \psi^*(\mathbf{x})) + \rho_0^{-1/2} \partial_x^2 \mathcal{V}_p(\mathbf{x}). \quad (40)$$

In Fourier space, this equation reads

$$[k^2(T + \tilde{\mathcal{V}}(k)) - i\mathbf{v}_p \cdot \mathbf{k} - \tau(\mathbf{v}_p \cdot \mathbf{k})^2] \tilde{\psi}^*(\mathbf{k}) = -\rho_0^{-1/2} k^2 \tilde{\mathcal{V}}_p(\mathbf{k}), \quad (41)$$

leading to the solution

$$\tilde{\psi}^*(\mathbf{k}) = \frac{-\rho_0^{-1/2} k^2 \tilde{\mathcal{V}}_p(\mathbf{k})}{k^2(T + \tilde{\mathcal{V}}(k)) - i\mathbf{v}_p \cdot \mathbf{k} - \tau(\mathbf{v}_p \cdot \mathbf{k})^2}. \quad (42)$$

Finally, the density variation in Fourier space is

$$\frac{\tilde{\delta\rho}^*(\mathbf{k})}{\rho_0} = \frac{-k^2 \tilde{\mathcal{V}}_p(\mathbf{k})}{k^2(T + \rho_0 \tilde{\mathcal{V}}(k)) - i\mathbf{v}_p \cdot \mathbf{k} - \tau(\mathbf{v}_p \cdot \mathbf{k})^2}. \quad (43)$$

### 5.2 Drag coefficient

The drag force can be expressed with the density variation in Fourier space as

$$\mathbf{F} = -\rho_0^{-1/2} \int i\mathbf{k} \tilde{\mathcal{V}}_p(\mathbf{k}) \tilde{\psi}^*(\mathbf{k}) \frac{d\mathbf{k}}{(2\pi)^d}, \quad (44)$$

$$= i\rho_0^{-1} \int \frac{k k^2 \tilde{\mathcal{V}}_p(\mathbf{k})^2}{k^2(T + \tilde{\mathcal{V}}(k)) - i\mathbf{v}_p \cdot \mathbf{k} - \tau(\mathbf{v}_p \cdot \mathbf{k})^2} \frac{d\mathbf{k}}{(2\pi)^d}, \quad (45)$$

$$= -\rho_0^{-1} \int \frac{k(\mathbf{v}_p \cdot \mathbf{k}) k^2 \tilde{\mathcal{V}}_p(\mathbf{k})^2}{[k^2(T + \tilde{\mathcal{V}}(k)) - \tau(\mathbf{v}_p \cdot \mathbf{k})^2]^2 + (\mathbf{v}_p \cdot \mathbf{k})^2} \frac{d\mathbf{k}}{(2\pi)^d}. \quad (46)$$

Decomposing the wavevector as  $\mathbf{k} = (k_{\parallel}, \mathbf{k}_{\perp})$  according to the velocity  $\mathbf{v}_p$  allows to write the force as

$$\mathbf{F} = -\rho_0^{-1} \mathbf{v}_p \int \frac{k_{\parallel}^2 k^2 \tilde{\mathcal{V}}_p(\mathbf{k})^2}{[k^2(T + \tilde{\mathcal{V}}(k)) - \tau(v_p k_{\parallel})^2]^2 + (v_p k_{\parallel})^2} \frac{d\mathbf{k}}{(2\pi)^d}. \quad (47)$$

The drag coefficient  $\lambda$  is defined by  $\mathbf{F} = -\lambda \mathbf{v}_p$ ; it reads

$$\lambda = \rho_0 \int \frac{k_{\parallel}^2 k^2 \tilde{\mathcal{V}}_p(\mathbf{k})^2}{[k^2(T + \rho_0 \tilde{\mathcal{V}}(k)) - \tau(v_p k_{\parallel})^2]^2 + (v_p k_{\parallel})^2} \frac{d\mathbf{k}}{(2\pi)^d}. \quad (48)$$

This expression is our main result.

### 5.3 Numerical computation

Our main results are Eq. 43 for the stationary bath density around the probe and Eq. 48 for the drag coefficient. We are interested in their dependence on the probe velocity in two cases:

- (i) the bath particles are point-like (i.e. much smaller than the probe),
- (ii) the bath particles are identical to the probe.

In the case (i), for the values of the wavevector  $\mathbf{k}$  that contribute to the integral in Eq. 48,  $\tilde{V}(\mathbf{k}) \simeq \tilde{V}(0)$ . This allows to define the effective diffusion coefficient of the bath,

$$D_{\text{bath}} = T + \rho_0 \tilde{V}(0), \quad (49)$$

that sets the relaxation time of the density field  $\rho(\mathbf{x}, t)$ . The Péclet number is defined as

$$\text{Pe} = \frac{v_p}{D_{\text{bath}}}; \quad (50)$$

it compares the velocity of the probe to the relaxation of the field density field [11]. Its definition also involves the size of the probe, which has been set to 1 here. Then, the density around the probe and the drag coefficient can be written:

$$D_{\text{bath}} \frac{\tilde{\delta\rho}^*(\mathbf{k})}{\rho_0} = \frac{-\mathbf{k}^2 \tilde{V}_p(\mathbf{k})}{\mathbf{k}^2 - i\text{Pe}k_{\parallel} - \tau D_{\text{bath}} \text{Pe}^2 k_{\parallel}^2} \quad (51)$$

and

$$D_{\text{bath}}^2 \lambda = \rho_0 \int \frac{k_{\parallel}^2 \mathbf{k}^2 \tilde{V}_p(\mathbf{k})^2}{\left[ \mathbf{k}^2 - \tau D_{\text{bath}} \text{Pe}^2 k_{\parallel}^2 \right]^2 + \text{Pe}^2 k_{\parallel}^2} \frac{d\mathbf{k}}{(2\pi)^d}. \quad (52)$$

With the appropriate normalization, these quantities depend only on the Péclet number and the inertial number  $\tau D_{\text{bath}}$ . The bath density is plotted on Fig. 2 for heavy bath particles ( $\tau D_{\text{bath}} = 100$ ) at different Péclet numbers. The drag coefficient is plotted as a function of the Péclet number on Fig. 3, for different values of the inertial number. These curves exhibit shear-thickening and resemble those obtained by numerical simulations in [13] (see Fig. 2a). This effect is due to inertia, as it disappears at low inertial numbers; in accordance with the conclusions of [13]. The density profiles differ strongly from those found in [23] where no inertia was present: inertia allows density waves to propagate through the bath leading to the cone visible for  $\text{Pe} = 0.2, 0.5$  on Fig. 2.

In the case (ii), the dynamics of the bath depends on the mode  $\mathbf{k}$  and no collective diffusion coefficient can be defined. The bath density is plotted on Fig. 4 for  $\rho_0 \epsilon = 1$ ,  $\tau = 100$ , and different probe velocities; it has the same structure as in the previous case. The drag coefficient is plotted as a function of the probe velocity on Fig. 5 for  $\rho_0 \epsilon = 1$  and different inertial times  $\tau$ , and on Fig. 6 for  $\tau = 1$  and different interaction strengths  $\rho_0 \epsilon$ . A shear-thickening regime emerges at large inertial times and large interaction strengths, consistently with our finding for point-like bath particles.

### 5.4 Timescales

We show that the different observed behaviors can be rationalized by comparing the different timescales involved in our process. We focus on the case (ii) where the bath particles are identical to the probe. The length scale probed by this microrheology measurement is the size of the probe,  $a_p = 1$ . Four timescales emerge in our analysis:

- The inertial timescale  $\tau_i = m/\lambda_s = \tau$ .

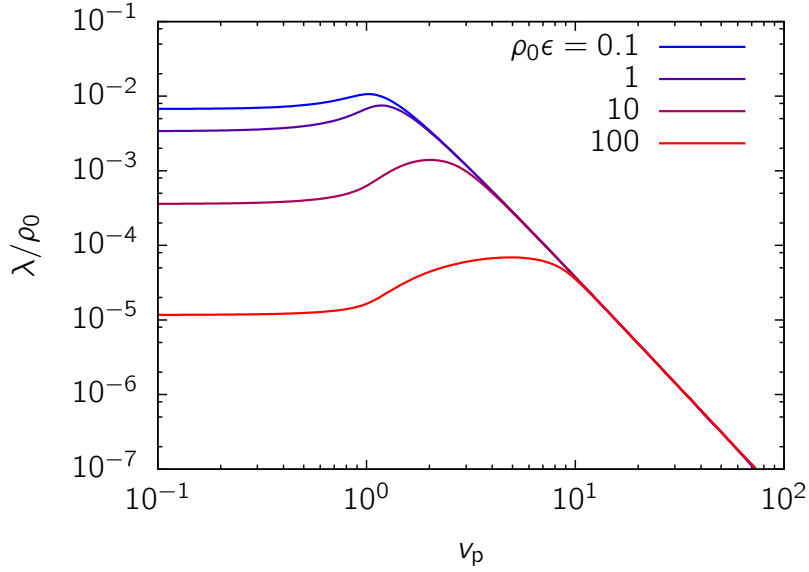


Figure 6: Friction coefficient as a function of the probe velocity when the bath particles are identical to the probe, for different values of the interaction strength  $\rho_0\epsilon$ , with  $\tau = 1$ . The friction coefficient is normalized by the density of the bath.

- The thermal diffusion timescale  $\tau_{\text{th}} = \lambda_s a_p^2 / T = 1$ ,
- The timescale associated with the density relaxation due to pair interactions,  $\tau_{\text{pair}} = \lambda_s / (\rho_0 a_p \epsilon) = 1 / (\rho_0 \epsilon)$ . The denominator,  $\rho_0 a_p^3 \epsilon$ , is the energy scale seen by one bath particle. This expression differs slightly from the one given in [13] for the viscous damping timescale ( $\tau_0$  in [13]), where  $\rho_0 \simeq a_p^{-3}$  and  $\tau_{\text{pair}} = \lambda_s a_p^2 / \epsilon$ .
- The timescale associated with the motion of the probe,  $\tau_p = a_p / v_p = 1 / v_p$ . In macrorheology, the characteristic timescale of the forcing is set by the shear rate  $\dot{\gamma}$ :  $\tau_{\text{shear}} = 1 / \dot{\gamma}$ .

At moderate density and low temperature, the suspension undergoes a glass transition [13]. We are interested in higher densities and temperatures, where the system still behaves as a fluid [32, 33, 34, 35]. In this case, thermal diffusion and pair interactions act together to relax the density; the first two terms on the r.h.s of Eq. 36 show that the two associated timescales  $\tau_{\text{th}}$  and  $\tau_{\text{pair}}$  are combined in one timescale  $\tau_{\text{rel}}$  related to the relaxation of the density field:

$$\frac{1}{\tau_{\text{rel}}} = \frac{1}{\tau_{\text{th}}} + \frac{1}{\tau_{\text{pair}}} = T + \rho_0 \epsilon. \quad (53)$$

Without inertia, i.e.  $\tau_i = 0$ , only two regimes are present (see Fig. 5,  $\tau = 0.1$ ): a Newtonian regime at small velocities where  $\tau_p > \tau_{\text{rel}}$ , and a shear-thinning regime at large probe velocities such that  $\tau_p < \tau_{\text{rel}}$ . The suspension shear thins because it does not have enough time to respond to the presence of the probe. This effect has already been evidenced in this framework in [23] and for a probe in more general environments in [31]. Shear-thinning regime is also observed in experiments [11, 12], numerical simulations [13, 16] and computations [18, 19, 21, 22]; it is due to the disruption of the static organization of the medium by the probe, which occurs when the forcing timescale becomes comparable to the relaxation timescale.

When inertia is added, expanding the denominator of the integrand in Eq. 48 for small probe velocities leads to the following criterion: shear-thickening is present if

$$\tau_i \gtrsim \tau_{\text{rel}}. \quad (54)$$

This is also the condition for the mode  $k = \pi/a_p$  of the density to oscillate and waves to develop in the wake of the probe (see Figs. 2 and 4).

A direct look at the same expression shows that the viscosity is maximal when

$$\tau_p \simeq \sqrt{\tau_i \tau_{\text{rel}}}, \quad (55)$$

which corresponds to a resonance between the forcing and the excited mode. This expression does not match the scaling found in [13] and explained by arguments from kinetic theory, which is  $\tau_p \simeq \tau_i^{3/4} \tau_{\text{rel}}^{1/4}$ . However, Kawasaki et al. suggest that the scaling (55) can be obtained assuming “soft particles and collisional dissipation”.

## 6 Conclusion

We considered a suspension of soft colloids with inertia and showed that the drag force on a probe pulled at constant velocity can be computed analytically in the limit of a dense suspension and soft colloids. The rheology of the suspension can be deduced: shear-thickening is observed if the inertia is high enough for density waves to propagate through the solution, in agreement with [13]. However, some quantitative differences arise between these numerical simulations and our computations in the scalings of the viscosity before the maximum and the position of the maximum. Numerical simulations closer to the regime that we studied, which are beyond the scope of this paper, would help to bridge this gap.

More generally, the ideal limit used here and already introduced in [23] without inertia proves to be a useful tool to investigate some non-linear rheological properties of colloidal suspensions. Indeed, simple analytical formulas can shed light on non-trivial physical phenomenon such as force induced diffusion [21, 23, 36, 37] or, here, inertia induced shear-thickening [13].

## Acknowledgments

I acknowledge financial support by the KECK foundation Award 37086.

## A Justification of the closure relation in the linearized equation

In this appendix, we rapidly justify the closure approximation (32) if density fluctuations are small, as in Subsec. 4.3.

Assuming that the local velocity distribution is the equilibrium velocity distribution shifted by an average velocity  $\bar{\mathbf{v}}(\mathbf{x}, t)$ , i.e.,

$$f(\mathbf{x}, \mathbf{v}, t) = \rho(\mathbf{x}, t) \left( 2\pi \frac{T}{\tau} \right)^{-d/2} \exp \left( -\frac{\tau[\mathbf{v} - \bar{\mathbf{v}}(\mathbf{x}, t)]^2}{2T} \right), \quad (56)$$

the current reads

$$\mathbf{j}(\mathbf{x}, t) = \rho(\mathbf{x}, t) \bar{\mathbf{v}}(\mathbf{x}, t), \quad (57)$$

and the second velocity moment is

$$\int \mathbf{v} \mathbf{v}^T f(\mathbf{x}, \mathbf{v}, t) d\mathbf{v} = \frac{T}{\tau} \rho(\mathbf{x}, t) \mathbf{1} + \bar{\mathbf{v}}(\mathbf{x}, t) \bar{\mathbf{v}}(\mathbf{x}, t)^T \rho(\mathbf{x}, t), \quad (58)$$

$$= \frac{T}{\tau} \rho(\mathbf{x}, t) \mathbf{1} + \frac{\mathbf{j}(\mathbf{x}, t) \mathbf{j}(\mathbf{x}, t)^T}{\rho(\mathbf{x}, t)}, \quad (59)$$

which is a generalization of the closure relation (32) used in the main text.

In Subsec. 4.3, the density fluctuations  $\delta\rho(\mathbf{x}, t) = \rho_0^{1/2}\psi(\mathbf{x}, t)$  are small compared to the average density  $\rho_0$ . As the average density is increased, we can assume that the current magnitude scales as the density fluctuations, i.e.  $j(\mathbf{r}, t) \sim \rho_0^{1/2}$ . The second term in Eq. 59 then scales as 1, which is small compared to the leading terms in Eq. 34, scaling as  $\rho_0^{1/2}$ . Thus, the correction to the closure relation does not affect the linearized equation (36).

## References

- [1] Jan Mewis and Norman J. Wagner. *Colloidal suspension rheology*. Cambridge University Press, 2011.
- [2] Philippe Coussot. *Rheometry of pastes, suspensions, and granular materials: applications in industry and environment*. John Wiley & Sons, 2005.
- [3] Atsushi Ikeda, Ludovic Berthier, and Peter Sollich. Unified study of glass and jamming rheology in soft particle systems. *Phys. Rev. Lett.*, 109(1):018301, Jul 2012.
- [4] Hans Martin Laun. Rheological properties of aqueous polymer dispersions. *Die Angewandte Makromolekulare Chemie*, 123(1):335–359, 1984.
- [5] Norman J. Wagner and John F. Brady. Shear thickening in colloidal dispersions. *Physics Today*, 62(10):27–32, 2009.
- [6] R. A. Bagnold. Experiments on a Gravity-Free Dispersion of Large Solid Spheres in a Newtonian Fluid under Shear. *Proceedings of the Royal Society of London A: Mathematical, Physical and Engineering Sciences*, 225(1160):49–63, 1954.
- [7] François Boyer, Élisabeth Guazzelli, and Olivier Pouliquen. Unifying Suspension and Granular Rheology. *Phys. Rev. Lett.*, 107(18):188301, Oct 2011.
- [8] T. A. Waigh. Microrheology of complex fluids. *Reports on Progress in Physics*, 68(3):685, 2005.
- [9] Todd M. Squires and Thomas G. Mason. Fluid Mechanics of Microrheology. *Annual Review of Fluid Mechanics*, 42(1):413–438, 2010.
- [10] Laurence G. Wilson and Wilson C. K. Poon. Small-world rheology: an introduction to probe-based active microrheology. *Phys. Chem. Chem. Phys.*, 13(22):10617–10630, 2011.
- [11] Alexander Meyer, Andrew Marshall, Brian G. Bush, and Eric M. Furst. Laser tweezer microrheology of a colloidal suspension. *Journal of Rheology*, 50(1):77–92, 2006.
- [12] Indira Sriram, Alexander Meyer, and Eric M. Furst. Active microrheology of a colloidal suspension in the direct collision limit. *Physics of Fluids (1994–present)*, 22(6), 2010.
- [13] Takeshi Kawasaki, Atsushi Ikeda, and Ludovic Berthier. Thinning or thickening?: Multiple rheological regimes in dense suspensions of soft particles. *EPL*, 107(2):28009, 2014.
- [14] M. Trulsson, M. Bouzid, J. Kurchan, E. Clement, P. Claudin, and B. Andreotti. Athermal analogue of sheared colloidal suspensions. *ArXiv e-prints*, nov 2014.
- [15] Martin Trulsson, Bruno Andreotti, and Philippe Claudin. Transition from the Viscous to Inertial Regime in Dense Suspensions. *Phys. Rev. Lett.*, 109(11):118305, Sep 2012.
- [16] Ileana C. Carpen and John F. Brady. Microrheology of colloidal dispersions by Brownian dynamics simulations. *Journal of Rheology (1978–present)*, 49(6):1483–1502, 2005.

- [17] D. Winter, J. Horbach, P. Virnau, and K. Binder. Active Nonlinear Microrheology in a Glass-Forming Yukawa Fluid. *Phys. Rev. Lett.*, 108(2):028303, Jan 2012.
- [18] Matthias Fuchs and Michael E. Cates. Theory of Nonlinear Rheology and Yielding of Dense Colloidal Suspensions. *Phys. Rev. Lett.*, 89(24):248304, Nov 2002.
- [19] Todd M. Squires and John F. Brady. A simple paradigm for active and nonlinear microrheology. *Physics of Fluids (1994-present)*, 17(7):073101, 2005.
- [20] Aditya S. Khair and John F. Brady. Single particle motion in colloidal dispersions: a simple model for active and nonlinear microrheology. *Journal of Fluid Mechanics*, 557:73–117, 6 2006.
- [21] Ch J. Harrer, D. Winter, J. Horbach, M. Fuchs, and Th Voigtmann. Force-induced diffusion in microrheology. *Journal of Physics: Condensed Matter*, 24(46):464105, 2012.
- [22] I. Gazuz and M. Fuchs. Nonlinear microrheology of dense colloidal suspensions: A mode-coupling theory. *Phys. Rev. E*, 87(3):032304, Mar 2013.
- [23] Vincent Démery, Olivier Bénichou, and Hugo Jacquin. Generalized Langevin equations for a driven tracer in dense soft colloids: construction and applications. *New Journal of Physics*, 16(5):053032, 2014.
- [24] Eric Brown and Heinrich M. Jaeger. Shear thickening in concentrated suspensions: phenomenology, mechanisms and relations to jamming. *Reports on Progress in Physics*, 77(4):046602, 2014.
- [25] Eric Brown and Heinrich M. Jaeger. Dynamic Jamming Point for Shear Thickening Suspensions. *Phys. Rev. Lett.*, 103(8):086001, Aug 2009.
- [26] John R. Melrose and Robin C. Ball. “Contact networks” in continuously shear thickening colloids. *Journal of Rheology (1978-present)*, 48(5):961–978, 2004.
- [27] J. Bergenholtz, J. F. Brady, and M. Vucic. The non-Newtonian rheology of dilute colloidal suspensions. *Journal of Fluid Mechanics*, 456:239–275, 4 2002.
- [28] Jan Mewis and Gary Biebaut. Shear thickening in steady and superposition flows effect of particle interaction forces. *Journal of Rheology (1978-present)*, 45(3):799–813, 2001.
- [29] David S. Dean. Langevin equation for the density of a system of interacting Langevin processes. *Journal of Physics A: Mathematical and General*, 29(24):L613–L617, 1996.
- [30] B. Øksendal. *Stochastic differential equations: an introduction with applications*. Springer, 5ème edition, 2000.
- [31] Vincent Démery and David S. Dean. Drag Forces in Classical Fields. *Phys. Rev. Lett.*, 104(8):080601, Feb 2010.
- [32] Frank H. Stillinger. Phase transitions in the Gaussian core system. *The Journal of Chemical Physics*, 65(10):3968–3974, 1976.
- [33] A. A. Louis, P. G. Bolhuis, and J. P. Hansen. Mean-field fluid behavior of the Gaussian core model. *Phys. Rev. E*, 62(6):7961–7972, Dec 2000.
- [34] Atsushi Ikeda and Kunimasa Miyazaki. Thermodynamic and structural properties of the high density Gaussian core model. *The Journal of Chemical Physics*, 135(2):024901, 2011.
- [35] Ludovic Berthier, Angel J. Moreno, and Grzegorz Szamel. Increasing the density melts ultrasoft colloidal glasses. *Phys. Rev. E*, 82(6):060501, Dec 2010.

- [36] Roseanna N. Zia and John F. Brady. Single-particle motion in colloids: force-induced diffusion. *Journal of Fluid Mechanics*, 658:188–210, 9 2010.
- [37] O. Bénichou, P. Illien, G. Oshanin, and R. Voituriez. Fluctuations and correlations of a driven tracer in a hard-core lattice gas. *Phys. Rev. E*, 87(3):032164, Mar 2013.